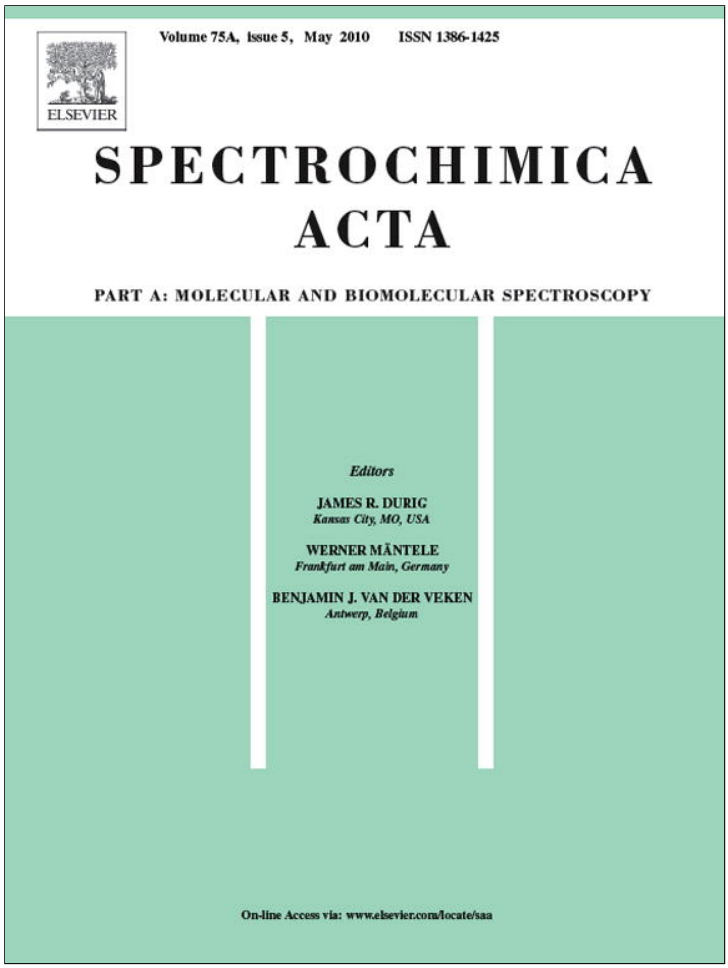

Spectrochimica Acta Part A 75 (2010) 1422–1434

Contents lists available at ScienceDirect

Spectrochimica Acta Part A: Molecular and Biomolecular Spectroscopy

journal homepage: www.elsevier.com/locate/saa

Theoretical and experimental vibrational spectrum study of 4-hydroxybenzoic acid as monomer and dimer

S.A. Brandán[a], F. Márquez López[b], M. Montejo[b], J.J. López González[b], A. Ben Altabef[a,*,1]

[a] INQUINOA, CONICET, Instituto de Química Física, Facultad de Bioquímica, Química y Farmacia, Universidad Nacional de Tucumán, San Lorenzo 456, T4000CAN Tucumán, Argentina
[b] Departamento de Química Física y Analítica, Facultad de Ciencias Experimentales, Universidad de Jaén, Campus de Las Lagunillas, Edif B-3, E-23071 Jaén, España, Spain

ARTICLE INFO

Article history:
Received 27 July 2009
Received in revised form
17 December 2009
Accepted 29 January 2010

Keywords:
4-hydroxybenzoic acid
Monomer
Dimer
Force field
SQM

ABSTRACT

Theoretical calculations on the molecular geometry and the vibrational spectrum of 4-hydroxybenzoic acid were carried out by the Density Functional Theory (DFT/B3LYP) method. In addition, IR and Raman spectra of the 4-hydroxybenzoic acid in solid phase were newly recorded using them in conjunction the experimental and theoretical data (including SQM calculations), a vibrational analysis of this molecular specie was accomplished and a reassignment of the normal modes corresponding to some spectral bands was proposed. The geometries of monomers and dimers in gas phase were optimized using the DFT B3LYP method with the 6-31G*, D95** and 6-311++G** basis sets. Also, both the vibrational spectra recorded and the results of the theoretical calculations show the presence of one stable conformer for the 4-hydroxybenzoic acid cyclic dimer. The B3LYP/6-31G* method was used to study the structure for cyclic dimer of 4-hydroxybenzoic acid and for a complete assignment our results were compared with results of the cyclic dimer of benzoic acid. A scaled quantum mechanical analysis was carried out to yield the best set of harmonic force constants. The formation of the hydrogen bond was investigated in terms of the charge density by the AIM program and by the NBO calculations.

1. Introduction

The 4-hydroxybenzoic acid is the simplest of the three components of the hydroxybenzoic series of the so named "polyphenols" belonging to the group of the minor constituents of olive oil, chemically unrelated with fatty acids [1]. The cell antioxidant action in living organisms, and especially in humans, of this type of compounds has been amply proved [2–4]. Hence, at present their bio-medical interest is clearly increasing for the prevention and treatment of cell ageing [5–7] and cardiovascular [8,9] and carcinogenic diseases [10–16], etc. In addition, the 4-hydroxybenzoic acid and some of their derivatives are of high industrial interest when preparing synthetic high polymers to be used in novel liquid crystals [17–20]. We think that a more thorough and better knowledge of the structural properties and of spectroscopic characteristics of this and other similar molecular species could help significantly form to get major advances in the above referred applications.

At this time, only a few references relative to the molecular structure [21–26], electronic structure and thermodynamic properties [27,28] and vibrational spectra of 4-hydroxybenzoic acid appear in the literature [22,29–31]. Thus, in 1986 Sánchez de La Blanca et al. [30,31] carried out an incomplete assignment of its vibrational spectrum by recording its IR and Raman spectra and with the help of group theory. In this way, they were able to assign 31 of the 42 vibrational normal modes expected for this molecule. From their results they proposed that the 4-hydroxybenzoic acid solid has intermolecular hydrogen bond. Later, a theoretical study of the structures and of the hydrogen bonds in the gas phase (*ab initio* quantum chemical calculations) and aqueous solution (Monte Carlo simulations for isothermal–isobaric ensembles) of the 2- and 4-hydroxybenzoic acids was realized by Nagy et al. [22]. In this last case the authors using the MP2 method with the basis set 6-31G*, accomplished a total geometry optimization of eight and four, theoretically possible planar conformers in phase gas respectively for the hydroxy-carboxylic derivatives above mentioned. They have also calculated the corresponding fundamental theoretical vibrational frequencies of all those conformers although without trying to carry out any assignment of their corresponding normal modes to the experimental vibrational spectra.

The crystal structure and molecular structural data from the solid phase of 4-hydroxybenzoic acid were firstly given by Colapietro et al. [24] by using X-ray diffraction. Later, Heath et al. [23] carried out a new experimental study and they showed that two molecules of the acid are linked through hydrogen bonds between their carboxylic groups thus a centre-symmetrical cyclic structure originated for the corresponding dimer. The benzenic ring has essentially hexagonal symmetry being its carbon atoms practically

* Corresponding author. Tel.: +54 381 4311044; fax: +54 381 4248169.
E-mail address: altabef@fbqf.unt.edu.ar (A. Ben Altabef).
[1] Member of the Carrera del Investigador Científico, CONICET, Argentina.

1386-1425/$ – see front matter © 2010 Elsevier B.V. All rights reserved.
doi:10.1016/j.saa.2010.01.012

coplanar while the hydrogen and oxygen atoms of the hydroxyl and carboxylic groups are only slightly deviated from the ring plane.

In order to get the best possible characterization and identification of the components of the hydroxybenzoic series of the "polyphenols", in this paper we carried out a more complete and reliable assignment of the vibrational spectra of 4-hydroxybenzoic acid. Thus, we first performed geometry optimization calculations for the monomer and cyclic dimer of 4-hydroxybenzoic acid using DFT/B3LYP methods with 6-31G*, D95** and 6-311++G** basis sets. Later, in order to assure a correct assignment of the experimental (IR and Raman) spectra of this molecule to its corresponding vibrational normal modes, we accomplished a theoretical/experimental analysis of vibrational spectra. Besides, calculations of the force constant associated to the main normal modes of vibration and the potential energy distribution with the scaled quantum mechanics (SQM) force field were performed. The total energies calculated with all basis sets for 4-hydroxybenzoic acid cyclic dimer were corrected for basis set superposition error (BSSE) by the standard Boys–Bernardi counterpoise method [32].

In addition, the frequency bands in the vibrational spectra of 4-hydroxybenzoic acid in solid phase could be supported with the theoretical calculations for the centrosymmetric dimeric species and with other papers reported in the literature for benzoic acid cyclic dimer [33–41] and o-hydroxybenzoic acid [42]. The topological AIM charge density analysis [43–45] and the NBO studies [46–49] for dimeric species show a characteristic structure of the OH stretching band typically associated with strong hydrogen bonds.

2. Experimental details

The 4-hydroxybenzoic acid was obtained from Sigma–Aldrich (99%) and was used without any further purification. The infrared spectra of the solid sample in KBr pellets at room temperature, in the range between 4000 and 400 cm^{-1} and with 1 cm^{-1} of resolution were registered on a Perkin Elmer 1760-X FTIR spectrophotometer. In addition, the Raman spectra of the solid samples, in the range between 4000 and 50 cm^{-1} and with a resolution of 1 cm^{-1}, were also registered at room temperature on a FT-Raman RF100/S Bruker spectrometer, using light of 1064 nm from an Nd/YAG laser for excitation.

3. Computational details

Initial structures for 4-hydroxybenzoic acid monomer and cyclic dimer were modelled with the GaussView Program [50] using Density Functional Theory. All the calculations were made using the GAUSSIAN 03 program [51] running on a Digital Alpha Server 4100. In vibrational studies of the benzoic acid monomer and dimer, various authors have examined the basis set dependence on the structural parameters and the infrared spectrum [34–39]. Hence, we have performed calculations for the geometries and harmonic frequencies in cartesian coordinates of monomer and cyclic dimer of 4-hydroxybenzoic acid using 6-31G*, D95** [52,53] and 6-311+G* basis sets. The resulting force field calculations were transformed to "natural" internal coordinates by the MOLVIB program [54,55]. The natural coordinates for 4-hydroxybenzoic acid monomer are shown in Table S1 of the Supporting Material and have been defined as proposed by Fogarasi and Pulay [56] and the definition of internal coordinates used is observed in Fig. 1. The natural coordinates for the cyclic dimer are the same as in the monomer for molecule in Fig. 1 following numeration of atoms from 17 to 32, as indicated in Fig. 2. Table S2 shows only the six intermonomer coordinates for the cyclic dimer, which are similar to those, defined by other authors for the benzoic acid dimer [36,37,39].

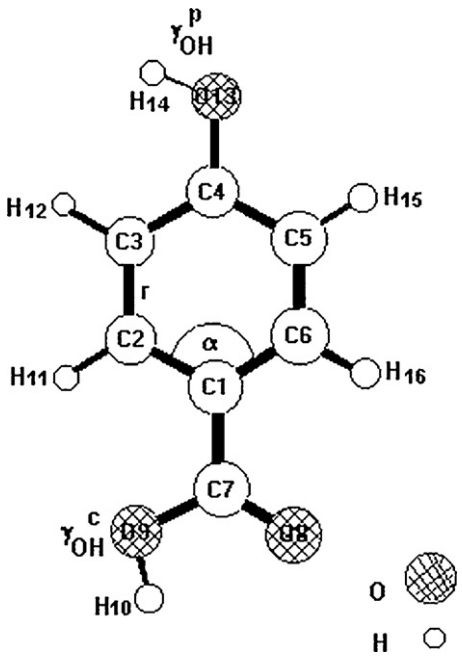

Fig. 1. Definition of internal coordinates for monomers of 4-hydroxybenzoic acid.

The force field was scaled using the transferable scale factors of Rauhut and Pulay [57–59] with the MOLVIB program. The potential energy distribution (PED) components greater than or equal to 10% are subsequently calculated with the resulting scaled quantum mechanics (SQM) force field.

The main stabilization energies were calculated by means of the Natural Bond Orbital (NBO) approach [46–49], as implemented in the GAUSSIAN 03 package, using the B3LYP/6-311++G** method. Moreover, at the same level of calculation the topological properties of the charge density for the cyclic dimer were computed by means of the AIM2000 program [44]. The total energies for cyclic dimers were corrected for basis set superposition error (BSSE) by the standard Boys–Bernardi counterpoise method [32].

4. Results and discussion

4.1. Geometry

The DFT calculations show the presence of four conformers of 4-hydroxybenzoic acid monomer, but only I and II conformers are stable (see Fig. 2), in accordance with the MP2 calculations by Nagy et al. [22]. The optimized geometries using B3LYP method with 6-31G*, D95** and 6-311+G* basis sets are observed in Table S3 and are compared with those experimental values obtained by Colapietro et al. [24]. We observed that the geometrical parameters of the monomer species using B3LYP method are not better than those obtained for Nagy et al. [22]. Obviously, the optimized bond lengths are longer than the experimental values because in the first case the calculations were carried out with the isolated molecules in gas phase whereas in the second one they were performed in solid phase.

For the calculations of the cyclic dimer we considered two structures, form I with the phenolic OH in the same position and form II in different position, as shown in Fig. 3. In all cases, planar structures for both monomers and cyclic dimer are predicted. The optimized structures with 6-31G*, D95** and 6-311+G* basis sets for two monomer species have C_1 symmetry whereas for cyclic dimer, I

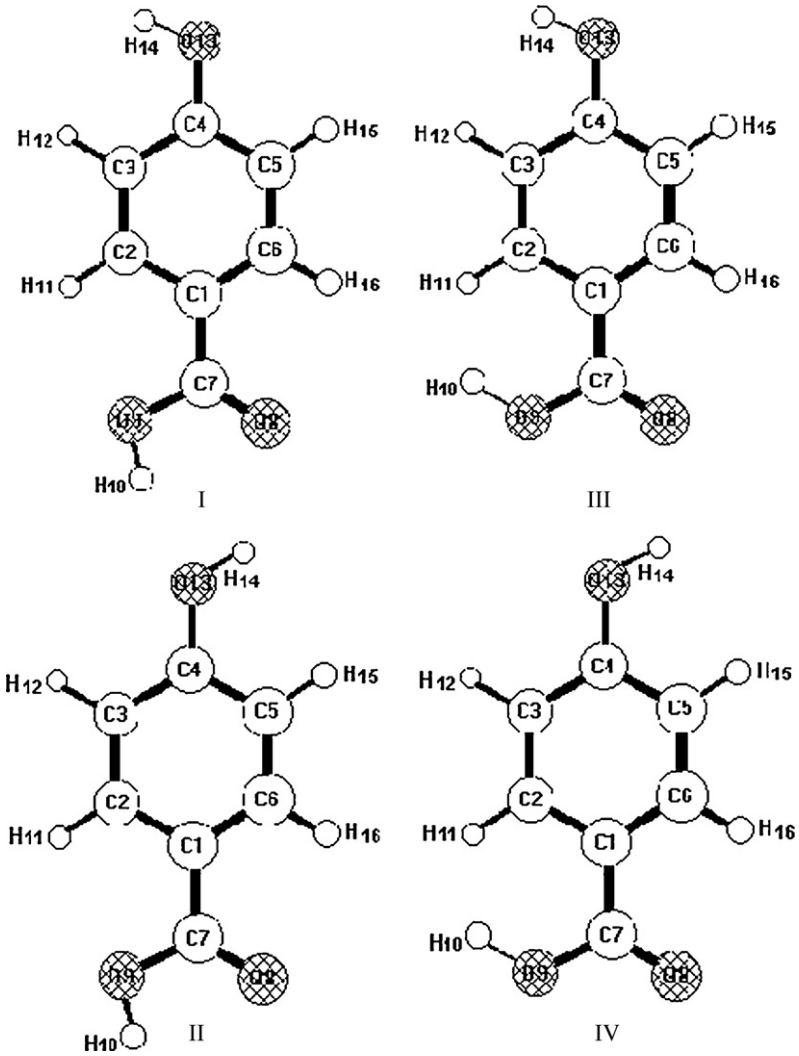

Fig. 2. Four conformers of 4-hydroxybenzoic acid.

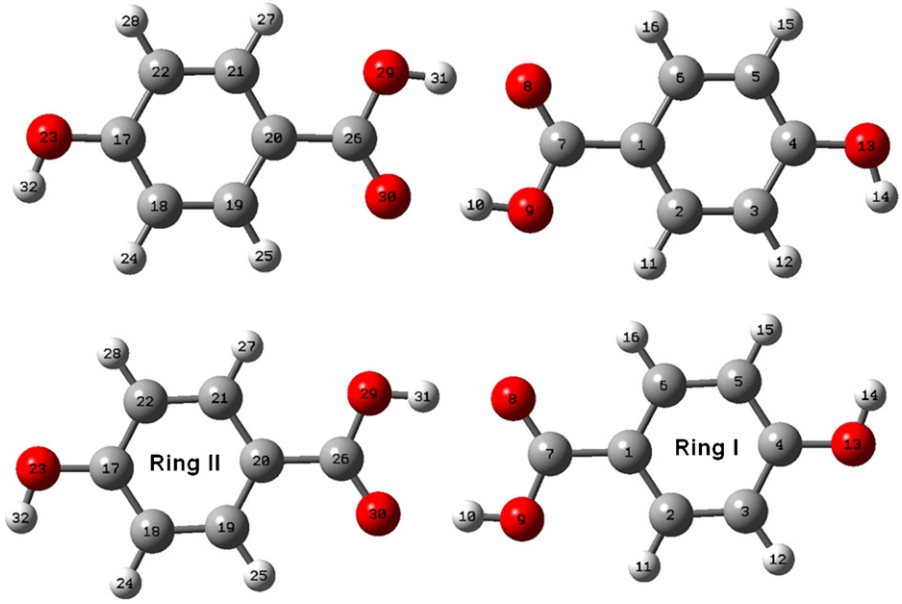

Fig. 3. Two conformers of 4-hydroxybenzoic acid cyclic dimer.

Table 1
B3LYP geometric parameters for 4-Hydroxybenzoic acid cyclic dimers compared with experimental geometrical parameters.

Cyclic dimers[a]							Ref.[b]	Ref.[c]	Ref.[d]
Geometric parameters	(I) Structure (C_s)			(II) Structure (C_{2h})					
	6-31G*	D95**	6-311++G**	6-31G*	D95**	6-311++G**			
Bond lengths (Å)									
R(1,2)	1.402	1.406	1.399	1.405	1.409	1.403	1.389	1.386	1.390
R(1,6)	1.405	1.408	1.402	1.401	1.406	1.399	1.394	1.385	1.393
R(1,7)	1.479	1.485	1.479	1.479	1.483	1.479	1.479	1.480	1.475
R(2,3)	1.390	1.396	1.389	1.388	1.394	1.386	1.381	1.382	1.386
R(2,11)	1.084	1.086	1.082	1.084	1.087	1.082	1.073		
R(3,4)	1.401	1.407	1.398	1.402	1.407	1.398	1.389	1.380	1.390
R(3,12)	1.088	1.099	1.086	1.085	1.088	1.083	1.074		
R(4,5)	1.402	1.407	1.399	1.402	1.408	1.399	1.391	1.385	1.394
R(4,13)	1.362	1.366	1.362	1.362	1.366	1.362	1.344		1.357
R(5,6)	1.386	1.393	1.384	1.389	1.396	1.387	1.378	1.383	1.387
R(5,15)	1.085	1.087	1.083	1.088	1.091	1.086	1.074		
R(6,16)	1.085	1.087	1.083	1.085	1.087	1.083	1.073		
R(7,8)	1.236	1.243	1.232	1.237	1.241	1.232	1.192	1.266	1.228
R(7,9)	1.326	1.325	1.324	1.325	1.328	1.324	1.332	1.266	1.322
R(9,10)	1.005	1.012	1.001	1.005	1.007	1.000	0.952		0.930
R(13,14)	0.970	0.968	0.963	0.970	0.970	0.963	0.947		0.840
Bond angles (°)									
A(2,1,6)	119.2	119.4	119.2	119.2	119.4	119.2		119.1	119.4
A(2,1,7)	121.8	121.4	121.7	121.9	121.6	121.8	118.4	120.1	119.4
A(6,1,7)	119.0	119.2	119.1	118.9	119.0	119.0		120.8	
A(1,2,3)	120.4	120.3	120.4	120.6	120.6	120.6	120.7	119.2	120.8
A(1,2,11)	119.5	119.4	119.5	119.3	119.3	119.3			
A(3,2,11)	120.1	120.2	120.0	120.0	120.1	120.0	120.3		
A(2,3,4)	119.8	119.7	119.8	119.7	119.6	119.6	119.6	120.7	
A(2,3,12)	120.2	120.2	120.1	121.4	121.5	121.3	120.3		
A(4,3,12)	120.0	120.0	120.1	118.9	118.9	118.9			
A(3,4,5)	120.2	120.3	120.3	120.2	120.3	120.3	120.4	121.0	120.5
A(3,4,13)	122.5	122.4	122.5	117.2	117.2	117.2		117.5	
A(5,4,13)	117.3	117.3	117.2	122.6	122.4	122.5		121.4	
A(4,5,6)	119.5	119.5	119.5	119.7	119.6	119.7	119.6	119.2	
A(4,5,15)	118.9	119.0	118.9	120.0	120.1	120.0	119.0		
A(6,5,15)	121.5	121.5	121.5	120.3	120.2	120.2			
A(1,6,5)	120.8	120.7	120.8	120.6	120.5	120.5	120.7	120.8	
A(1,6,16)	118.6	118.7	118.7	118.8	118.9	118.9			
A(5,6,16)	120.6	120.5	120.5	120.6	120.6	120.5	119.6		
A(1,7,8)	122.1	121.9	122.3	122.1	122.2	122.4	124.8	118.6	123.2
A(1,7,9)	114.4	114.8	114.6	114.4	114.6	114.5	113.5	118.2	114.7
A(8,7,9)	123.5	123.3	123.1	123.5	123.2	123.1		123.2	
A(7,9,10)	108.9	110.0	110.3	109.9	109.5	110.3	107.6		109
A(4,13,14)	109.2	109.3	110.0	109.2	109.2	110.0	111		112

[a] This work.
[b] Ref. [22].
[c] Ref. [23].
[d] Ref. [24].

structure has C_s symmetry and its corresponding II structure has C_{2h} symmetry. The geometrical parameters for both structures of cyclic dimers using all calculations are given in Table 1 compared with observed values by other authors [22,24]. The geometrical parameters for the three levels of calculations of dimeric specie that participate in the hydrogen bond are presented in Table 2 compared with theoretical values for benzoic acid dimer. In general, the best agreement in the calculated bond lengths with the 6-31G* basis set is obtained. When we examined the basis set dependence on the geometrical parameters for the cyclic dimers in reference to monomers, an increase in the basis set size from 6-31G* to D95** or 6-311+G** a small decrease in the bond angles is observed whereas the bond lengths practically do not change. This fact is similar to that observed by Urbanová et al. [38] for the benzoic acid dimer as can be seen in the same table. These results show that the B3LYP/6-311++G** geometry presents the best overall agreement with those values obtained for benzoic acid dimer at the same level calculation.

The relative energy in kJ/mol and dipole moment for 4-hydroxybenzoic acid monomers is observed in Table 3 at different levels of theory together with the corresponding values of relative energies uncorrected for basis set superposition error effects for the cyclic dimers. The values of barrier to interconversion between two monomers are 0.26, 0.2516 and 0.2361 kJ/mol using 6-31G*, D95** and 6-311+G* basis sets respectively, while the values of barrier to interconversion between the two cyclic dimers using 6-31G*, D95** and 6-311++G** basis sets is 0.0566, 0.0886 and 0.0244 kJ/mol respectively. The theoretical values of dipole moments for all conformers are also observed in the same Table. These dipole moment values for two monomers are in accordance with those obtained previously for this compound by Nagy et al. using HF/6-31G* method [22]. The dipole moment values for the II structures (monomer and cyclic dimer) with the three basis sets are lower than the other values. This behavior is similar to calculation results obtained by Antony et al. [33] for the benzoic acid monomer and dimer. These authors find that the dipole moment value using D95** basis set is 2.06 D whereas when using cc-pVTZ base set it is 2.03 D for the monomer. For the cyclic dimer with the two basis sets, above mentioned, the values are 0.0078 and 0.0 D, respectively. In that case, the energy difference between the equilibrium cyclic dimer and the two isolated monomers of benzoic acid

Table 2
B3LYP geometric parameters for 4-hydroxybenzoic acid monomers and cyclic dimer compared with parameters of benzoic acid monomer and cyclic dimer[a].

	4-Hydroxybenzoic acid[b]												Benzoic acid[a]			
	Monomers						Cyclic dimer						Mon.	Cyclic dimer		
	I			II			I			II						
	6-31G*	D95**	c,b	6-31G*	D95**	c	6-31G*	D95**	c,b	6-31G*	D95**	c	6-31G*	6-31G*		c
Bond lengths (Å)																
C=O	1.216	1.220	1.186	1.217	1.220	1.212	1.236	1.243	1.232	1.237	1.241	1.232	1.215	1.235	1.235	1.230
O–H	–	–	–	–	–	–	1.671	1.649	1.655	1.671	1.647	1.660	–	1.673	1.673	1.662
O–O	–	–	–	–	–	–	2.675	2.656	2.656	2.676	2.655	2.660	–	2.677	2.677	2.662
H–O	0.975	0.973	0.944	0.975	0.973	0.969	1.005	1.012	1.001	1.005	1.007	1.000	0.975	1.005	1.005	1.000
C–O	1.361	1.365	1.330	1.361	1.364	1.360	1.325	1.325	1.324	1.325	1.328	1.324	1.359	1.324	1.324	1.323
C–C	1.479	1.484	1.479	1.479	1.484	1.478	1.479	1.485	1.479	1.479	1.483	1.479	1.487	1.486	1.486	1.486
Bond angles (°)																
C=O–H	–	–	–	–	–	–	124.9	126.7	126.4	124.9	126.7	126.7	–	125.0	126.8	
O–H–O	–	–	–	–	–	–	178.4	179.3	179.9	178.3	179.4	179.9	–	178.6	179.6	
H–O–C	105.3	105.6	108.4	105.4	105.7	106.5	109.9	110.0	110.3	109.9	109.5	110.3	105.5	109.9	110.3	
O–C=O	121.6	121.7	121.7	121.7	121.7	121.4	123.5	123.3	123.1	123.5	123.2	123.1	121.8	123.6	123.3	

[a] Ref. [38].
[b] This work.
[c] 6-311++G**.

with D95** basis set is 19.14 kcal/mol and with the cc-pVTZ base set it is 17.21 kcal/mol. Reva and Stepanian [41] predict an energy difference between the equilibrium cyclic dimer and the two isolated monomers of benzoic acid (using *ab initio* 4-31G results) as 21.2 kcal/mol while the energy difference between their monomers is 9.6 kcal/mol. Stepanian et al. [40] also reported the same value with the AM1 method for the barrier between *Syn* (I) → *Anti* (II) transition for the two monomers of benzoic acid. Urbanová et al. [38] predict that the barrier to interconversion with B3LYP/6-31G* method, for the same conformers of benzoic acid dimer is 7.7 kcal/mol. This energy difference was taken into account for the interpretation of the infrared spectrum of benzoic acid. It is important to note that the total energy for 4-hydroxybenzoic acid cyclic dimer is smaller than the sum of the energies of each monomer. Such observation could mean that the presence of the dimers even in gas phase is preferable to the isolated monomer. This result is very important and it will be taken into consideration in the assignment of the vibrational spectra registered for this compound.

Table 4 shows the total energy values for the two cyclic dimers uncorrected ($^{\&}E$) and corrected ($^{\#}E$) for BSSE effects using the counterpoise method with B3LYP method at different levels of theory. The energy values for the II structures are more stable than the corresponding I structures. A comparison of the results between 6-31G* and 6-311++G** basis sets indicates a large effect of the diffuse functions on the total energies at the correlated level (6-31G*) and these functions will reduce the effect of BSSE lowering the magnitude of the total energies. The BSSE value for the II structure is negligible with the larger basis set (6-311++G**) as can be seen in Table 4.

4.2. Topological analysis

Numerous authors have studied the hydrogen bonds associated with the appearance of bond critical points between the hydrogen atom and the acceptor atom, which are linked by the bond path [45,60]. In the 4-hydroxybenzoic acid cyclic dimer the presence of two hydrogen bonds such as OH–O is studied by means of topological analysis and evaluation of all local properties using the AIM2000 program [43,44]. For a correct characterization of the H bond, the calculations were carry out only at B3LYP/6-311++G** level. The molecular models for I and II cyclic dimers are observed in Fig. 3.

Table 5 shows the critical points localized in both dimeric structures using the 6-311++G** basis set. Two hydrogen bonds (for I and II structures) with the same properties were localized. Where $\rho(r)$ is the electron density and $\nabla^2\rho(r)$ is the Laplacian of the electron density. It is positive when the interaction is dominated by the contraction of charge away from the interatomic surface toward each nucleus. The values $\lambda1$, $\lambda2$ and $\lambda3$ are three eigenvalues obtained from the diagonalization of the Hessian of the electron density, ordered in following order: $\lambda1 < \lambda2 < \lambda3$ and moreover $|\lambda1|/\lambda3 < 1$. The values obtained are well characterized for the criteria proposed by Koch et al. [45]. The same values of $\rho(r)$ for the two structures and with the same basis set suggest that the different position of OH phenolic group do not affect the characteristics of the H bond. The eight critical points and the ring point of the electron density obtained by AIM analysis clearly reveal the formation of hydrogen bonds among two COOH groups of the monomers, as shown in Fig. 4.

4.3. NBO analysis

The 4-hydroxybenzoic acid cyclic dimer was also studied by means of the NBO analysis. In this case, the electronic wavefunction is interpreted in terms of a set of occupied Lewis and a set unoccupied non-Lewis localized orbitals and the delocalization effects can be identified by the presence of off-diagonal elements of the

Table 3
Relative energy ((*E*) and dipole moment (μ) for 4-hydroxybenzoic acid monomers and cyclic dimers at different levels of theory.

	B3LYP method						
	6-31G*		D95**		6-311++G**		
	(E^a (kJ/mol)	μ^a (D)	(E^a (kJ/mol)	μ^a (D)	(E^a (kJ/mol)	μ^a (D)	μ^b (D)
Monomer							
I	0.2600	3.12	0.2516	3.35	0.2361	3.35	3.38
II	0.0000	1.74	0.0000	1.92	0.0000	1.93	1.66
Cyclic dimmer							
I	0.0566	2.72	0.0886	2.75	0.0244	2.75	–
II	0.0000	0.00	0.0000	0.36	0.0000	0.47	–

[a] This work.
[b] Ref. [22].

Table 4
The total energies values uncorrected ($^{\&}E$) and corrected ($^{\#}E$) for BSSE effects using the counterpoise method and the relative energy (ΔE) of the two cyclic dimers using different levels of theory.

	B3LYP method					
	(I) Structure			(II) Structure		
	6-31G*	6-311++G**	D95**	6-31G*	6-311++G**	D95**
$^{\&}E$ (a.u.)	−992.11306660	−992.42185550	−992.31676400	−992.11308820	−992.42184620	−992.3167302
$^{\#}E$ (a.u.)	−992.10665345	−992.42051304	−992.31331075	−992.10666394	−992.42176897	−992.31327579
ΔE (kJ/mol)	16.82	3.52	9.06	16.85	0.20	9.06

Fock matrix. The forces of these delocalization interactions, $E^{(2)}$ in kcal/mol, are estimated by the second-order perturbation theory. Also the sum $E^{(2)}$ terms corresponding to these interactions can be considered to be the total charge transfer energy. In this case the oxygen lone pairs LP(1) would be donors in intermolecular charge transfer interactions while the O–H antibonds (σ*) participate as acceptors. The occupancies of the orbital antibonds involved in the H bond of the cyclic dimer for two conformers with 6-311++G** basis set are given in Table 6. The electronic population observed in the σ*C7–O8 and σ*C26–O30 orbitals for the two dimeric structures indicate that they are receiving charge transfer. Whereas, the electronic occupations in the LP(1)O8 and LP(1)O30 orbitals have diminished the initial value of 2 (in the monomer) as observed in Table 6. The stabilization energies (in kcal/mol) associated with delocalizations from lone pairs to σ*O–H bond orbital of 4-hydroxybenzoic acid cyclic dimer are observed in Table 7. In the o-hydroxybenzoic case [42] the interactions of the calculations with B3LYP/6-31G* are lowers than the sum of our values: 14.71 and 16.63 kJ/mol (total energy equal to 31.34 kJ/mol). In the o-hydroxybenzoic case the change in the position of COOH group

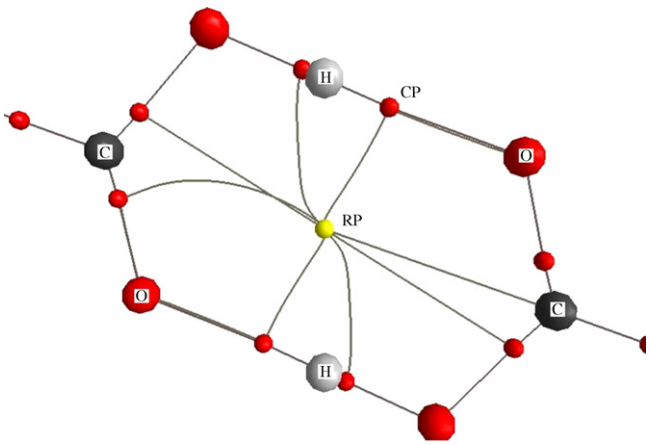

Fig. 4. The critical points of the charge density for 4-hydroxybenzoic acid cyclic dimer.

Table 5
Analysis of O–H bond critical points in 4-hydrybenzoic cyclic dimers. (The quantities are in atomics units.).

Bond	B3LYP/6-311++G**			
	I		II	
	O8–H31	O30–H10	O8–H31	O30–H10
$\rho(r)$	0.0489	0.0489	0.0484	0.0484
$\nabla^2\rho(r)$	0.1401	0.1401	0.1394	0.1394
λ1	−0.0879	−0.0879	−0.0864	−0.0864
λ2	−0.0860	−0.0860	−0.0845	−0.0845
λ3	0.3141	0.3140	0.3104	0.3104
|λ1|/λ3	0.2799	0.2799	0.2783	0.2783
Calculated	1.6558	1.6560	1.6604	1.6604
O···H (Å)	1.656	1.656	1.660	1.660
O···O (Å)	2.656	2.656	2.660	2.660

Experimental values [24]: O–H: 1.730 Å; O–O: 2.658 Å.

obviously changes the properties of the cyclic dimer due to the possible presence of another intramolecular H bond formation. These results are in excellent agreement with the topological analysis of the previous section and demonstrate the presence of the H bond between two units of monomer 4-hydroxybenzoic acid, as was experimentally observed in the solid state.

Table 6
The occupancies of the antibonding orbitals involved in the H bond of the two cyclic dimers.

Orbital	B3LYP/6-311++G**	
	Occupancy	
	(I) Structure	(II) Structure
σ*C7–O8	0.02534	0.02403
σ*C7–O8	0.31328	0.31335
LP(1)O8	1.95485	1.95738
LP(2)O8	1.85350	1.85357
σ*C26–O30	0.02414	0.02409
σ*C26–O30	0.31418	0.31335
LP(1)O30	1.95700	1.95746
LP(2)O30	1.85317	1.85355

4.4. Force field

Following the SQM procedure [57–59], the harmonic force field for the more stable 4-hydroxybenzoic acid cyclic dimer evaluated at B3LYP/6-31G* was scaled transferring the recommended scaled factors of Rauhut and Pulay [57,58]. The resulting scaled frequencies are shown in Table 8 together with the potential energy distribution and the assignment proposal by the theoretical calculation (Table S4). We can see that only 44 of the 90 modes of the cyclic dimer have participation ≥30% of one defined coordinate, whereas the other modes represent very complex vibrations where several coordinates are involved. When increasing the basis set size (6-31G*, D95** and 6-311++G**) we observed an increase in the intensity of the bands and a shifting of the bands towards lower wavenumbers as shown in Table S5. This fact is similar to that was observed by Urbanová et al. [38] in the benzoic acid dimer. The Rauhut–Pulay scale factors values [57,58] used are collected in Table S6 compared with the corresponding factors obtained by Stepanian et al. [40] for benzoic acid. In the benzoic acid cyclic dimer [33–41], the main couplings are: the Davydov coupling between the two localized OH stretch vibrations, Fermi coupling between the OH stretch and nearly resonant combination bands, and the coupling between OH stretch and interdimer H-bond vibrations. The greater difference found in that dimer is the strong shift of the CO–OH out-of-plane bending vibration (γ) from 571 cm^{-1} in the monomer to 962 cm^{-1} in the dimer caused by an effective shifting of the bending motion due to the hydrogen bond [35]. In that case, the harmonic shifted using D95** basis set is of 594 cm^{-1} in the monomer to 1003 and 1050 cm^{-1} in the dimer [33]. In this molecule, the harmonic frequencies obtained with the B3LYP/6-31G* and B3LYP/D95** methods differ notably for a few modes among them (about from 3 to 96 cm^{-1}) mainly in the monomers related to COOH group whereas in the cyclic dimer the situation is similar to dimer of benzoic acid. For 4-hydroxybenzoic acid cyclic dimer with the 6-31G*and D95** basis sets the CO–OH out-of-plane bending vibration undergoes shifting from 600 cm^{-1} in the monomer to 961 cm^{-1} in the dimer.

Table S7 summarizes the most important force constants from B3LYP/6-31G* calculation for 4-hydroxybenzoic acid cyclic dimer. The C=O stretching force constant presents slightly the greater value in the cyclic dimer, as expected. The force constant values corresponding to OH phenolic group for the cyclic dimer (f(γC–O), f(βC–O), f(βC–C)), practically does not change, due to the hydrogen bond formation is carried out by COOH group. Table S8 shows the main force constants of interaction involving the C=O and O–H stretching since the two groups are H-bonded to one another for the most stable conformer of 4-hydroxybenzoic acid cyclic dimer. The force field in natural coordinates is available from the authors on request.

5. Vibrational analysis

The dimer, $(C_7O_3H_6)_2$. The (I) structure of 4-hydroxybenzoic acid cyclic dimer has C_s symmetry planar and 90 normal vibrations and all vibrations are IR and Raman active including 61 A′ (planar) + 29 A″ (out-of-plane). The (II) structure of the cyclic dimer also has a planar structure but with C_{2h} point group. The total number of normal vibrations is 90 including 31 A_g (planar) + 30 B_u (planar) + 15 A_u (out-of-plane) + 14 B_g (out-of-plane). The A_u and B_u, vibrations are IR active while the A_g and B_g ones are Raman active. The IR and Raman spectra for 4-hydroxybenzoic acid in the solid phase appear in Figs. 5 and 6 respectively whereas the observed vibrational frequencies are collected in Table 8. The assignment of the vibrational modes of 4-hydroxybenzoic acid is based on the potential energy distribution (PED) obtained for the (II) structure of cyclic dimer from the B3LYP/6-31G* calculations (lowest energy). It should be emphasized that these three theoretical methods yielded almost identical or very similar PED values for the 90 corresponding normal modes of 4-hydroxybenzoic acid cyclic dimers. The comparison between the calculated values of frequencies for cyclic dimers is presented in Table S5 while the final assignments of the corresponding 90 normal vibration modes are presented in Table 8. For a complete assignment the calculated frequencies values for cyclic dimer were compared with values obtained for others authors for the benzoic acid cyclic dimer [33–41], with the available values for the phenol [61,62] and with the existent partial assignment for this molecule [30,31].

In the spectrum of benzoic acid Florio et al. [35,36] have observed important splittings of the bands involving motion of the entire COOH group: C=O stretch (1698/1657 cm^{-1}), the highly mixed OH bends (1458/1453/1444/1422/1288/1282 cm^{-1}), the O–C=O bend (792/781 and 656/647 cm^{-1}), (533/498 cm^{-1}) and the (426/388, 285/258 cm^{-1}). In the vibrational spectrum

Table 7
Stabilization energies ($E^{(2)}$) associated with delocalizations from lone pairs and delocalizations to σ*O–H bond orbital of 4-hydroxybenzoic acid cyclic dimers.

Orbital	B3LYP/6-311++G**	
	$E^{(2)}$ (kcal/mol)	
	(I) Structure	(II) Structure
LP(1)(O8) → σ*(O29–H31)	8.80	8.78
LP(2)(O8) → σ*(O29–H31)	21.99	21.56
LP(1)(O30) → σ*(O9–H10)	8.79	8.78
LP(2)(O30) → σ*(O9–H10)	22.13	21.56

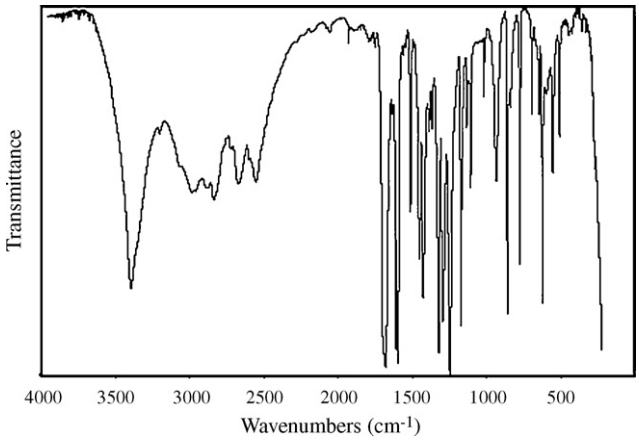

Fig. 5. The IR spectrum of solid normal 4-hydroxybenzoic acid at room temperature between 4000 and 400 cm^{-1}.

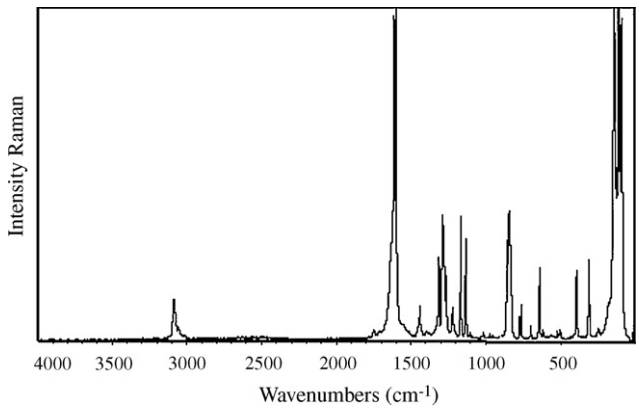

Fig. 6. The Raman spectrum of solid normal 4-hydroxybenzoic acid.

Table 8
Observed and calculated wavenumbers (cm^{-1}), potential energy distribution and assignment for structure II of dimer $(C_7H_6O_3)_2$.

Mode	Experimental				[a]B3LYP/6-31G*	[a]PED
	[a]IR (Sol)	[a]Raman (Sol)	[b]IR (Sol)	[b]Raman (Sol)	[c]SQM	(>10%)
A_g symmetry						
1	3395 s		3385 m		3591	ν (O13–H14) (100)
2	3202 vvw	3194 vvw			3103	ν (C21–H27) (45), ν (C2–H11) (39)
3		3160 vvw			3096	ν (C6–H16) (97)
4		3149 vvw			3084	ν (C21–H27) (43), ν (C2–H11) (41)
5		3087 m			3043	ν (C5–H15) (97)
6		3054 m			2956	ν (O13–H14) (92)
7	1614 vs	1613 vs		1620 m	1645	ν (C7═O8) (58)
8	1600 vs	1600 vs	1606 s	1607 s	1612	ν (C18–C19) (20), ν (C2–C3) (20)
9	1600 vs	1600 vs	1606 s	1607 s	1583	ν (C17–C18) (19), ν (C1–C2) (19), ν (C3–C4) (13), ν (C19–C20) (13)
10	1511 m			1508 m	1515	β (C18–H24) (13), β (C5–H15) (13), β (C21–H27) (11), β (C2–H11) (11)
11	1453 m	1455 βr, sh	1446 m	1450 vw	1444	δ (O9–H10) (15), ν (C7–O9) (12)
12	1428 s		1423 s		1429	δ (O9–H10) (14), ν (C7═O8) (11)
13	1320 vs	1315 m	1315 sh	1320 w	1338	δ (O13–H14) (12), ν (C2–C3) (12), ν (C1–C2) (12), ν (C18–C19) (12), ν (C17–C18) (12), ν (C1–C6) (11)
14	1320 vs	1315 m			1313	β (C18–H24) (15), β (C5–H15) (15), β (C21–H27) (11), β (C2–H11) (11)
15	1297 s	1290 s	1291 vs	1297 m	1274	ν (C4–O13) (30), ν (C1–C6) (18)
16	1245 vs		1243 vs		1269	ν (C4–O13) (21), ν (C7–O9) (18), ν (C1–C7) (14), δ (O9–H10) (11)
17		1223 w	1230 w	1231 w	1168	β (C5–H15) (19), β (C18–H25) (19), β (C2–H11) (16), β (C21–H28) (16)
18	1166 s	1166 s	1167 s	1174 m	1155	δ (O13–H14) (53)
19	1133 w	1132 m	1127 m	1140 m	1120	ν (C7–O9) (22), ν (C1–C7) (14)
20	1107 m	1104 vw	1100 m		1099	β (C21–H28) (15), β (C2–H11) (14), β (C18–H25) (12), ν (C18–C19) (12), β (C5–H15) (12), ν (C2–C3) (11)
21	1020 w	1017 vw	1012 w		1000	$\beta_{R1(II)}$ (26), $\beta_{R1(I)}$ (25)
22	832 sh	833 sh		829 w	828	ν (C4–O13) (13), ν (C17–C18) (11), ν (C1–C2) (11), ν (C19–C20) (11), ν (C3–C4) (11)
23	773 s	774 w			738	δ (C7–O8–O9) (16), δ (C26–O29–O30) (16), ν (C1–C7) (12)
24	644 w	643 w	640 vw	650 w	636	$\beta_{R3(II)}$ (38), $\beta_{R3(I)}$ (38)
25	620 s	622 vvw			598	δ (C7–O8–O9) (21), δ (C26–O29–O30) (21), $\beta_{R2(I)}$ (13), $\beta_{R2(II)}$ (13)
26		521 vvw			519	ρ (C1–C7–O8) (25), ρ (C20–C26–O30) (25)
27	401 vvw				402	β (C17–O23) (30), β (C4–O13) (30)
28		392 w			383	ν (O30–H10) (30), $\beta_{R2(II)}$ (15), $\beta_{R2(I)}$ (15), ν (C1–C7) (11)
29		243 sh			240	ν (C26–C20) (22), β (C7–C1) (22), δ (O30–H10) (21), δ (O9–H10) (15)
30		111 vs			106	ν (O30–H10) (63), δ (O30–H10) (18)
31		94 s			93	δ (O30–H10) (37), δ (O9–H10) (24), ν (C26–C20) (11), β (C7–C1) (11)
Bu symmetry						
32	3395 s		3385 m		3591	ν (O23–H32) (100)
33	3202 vvw	3194 vvw			3103	ν (C3–H12) (45), ν (C22–H28) (39)
34		3160 vvw			3096	ν (C19–H25) (97)
35		3149 vvw			3084	ν (C3–H12) (43), ν (C22–H28) (41)
36		3087 m			3050	ν (O29–H31) (85)
37		3054 m			3042	ν (C18–H24) (86), ν (O29–H31) (12)
38	1678 vs		1675 vs		1692	ν (C26═O30) (64)
39	1614 vs	1613 vs			1611	ν (C5–C6) (20), ν (C21–C22) (20)
40	1600 vs	1600 vs	1606 s	1607 s	1583	ν (C4–C5) (19), ν (C20–C21) (19), ν (C22–C17) (13), ν (C1–C6) (13)
41	1511 m		1508 m		1516	β (C6–H16) (13), β (C18–H24) (13), β (C2–H11) (11), β (C21–H27) (11)
42	1453 m	1455 βr, sh			1436	ν (C21–C22) (18), ν (C5–C6) (18)
43	1428 s				1403	δ (O29–H31) (38), ν (C26–O29) (23), ν (C20–C26) (15)
44	1320 vs	1315 m	1315 sh	1320 w	1338	δ (O23–H32) (12), ν (C21–C22) (12), ν (C20–C21) (12), ν (C5–C6) (12), ν (C4–C5) (12), ν (C22–C17) (11)
45	1320 vs	1315 m	1315 sh	1320 w	1313	β (C6–H16) (15), β (C18–H24) (15), β (C2–H11) (11), β (C21–H27) (11)
46	1297 s	1290 s	1291 vs	1297 m	1275	ν (C17–O23) (30), ν (C26–O29) (12)
47	1245 vs		1243 vs		1268	δ (O29–H31) (24), ν (C17–O23) (21), ν (C26–O29) (12), ν (C20–C26) (11)
48	1173 sh				1166	β (C18–H25) (20), β (C6–H6) (20), β (C21–H28) (15), β (C3–H12) (15)

Table 8 (*Continued*)

Mode	Experimental				[a]B3LYP/6-31G*	[a]PED
	[a]IR (Sol)	[a]Raman (Sol)	[b]IR (Sol)	[b]Raman (Sol)	[c]SQM	(>10%)
49	1166 s	1166 s	1167 s	1174 m	1154	δ (O23–H32) (52)
50	1133 w	1132 m	1127 m	1140 m	1117	ν (C26–O29) (22), ν (C20–C26) (14)
51	1107 m	1104 vw	1100 m		1099	β (C3–H12) (15), β (C21–H28) (14), ν (C5–C6) (12), β (C6–H6) (12), β (C18–H25) (12), ν (C21–C22) (11)
52	1020 w	1017 vw	1012 w		999	$\beta_{R1(I)}$ (26), $\beta_{R1(II)}$ (25)
53	856 s	855 m	853 s		850	γ (C2–H11) (25), γ (C21–H27) (24)
54	764 sh	765 w			760	γ (C7–O8–O9) (17), γ (C26–O29–O30) (17), $\tau_{R1(I)}$ (15), $\tau_{R1(II)}$ (15)
55	644 w	643 w	640 vw	650 w	636	$\beta_{R3(I)}$ (38), $\beta_{R3(II)}$ (38)
56	596 vvw				601	δ (C26–O29–O30) (18), δ (C7–O8–O9) (18), $\beta_{R2(II)}$ (16), $\beta_{R2(I)}$ (16)
57	550 m	544 vvw	546 m		550	((C20–C26–O30) (26), ((C1–C7–O8) (26), ν (O30–H10) (15)
58	409 vw				411	$\tau_{R3(II)}$ (46), $\tau_{R3(I)}$ (31)
59	357 vvw	355 vvw			343	ν (C20–C26) (25),$\beta_{R2(I)}$ (24), $\beta_{R2(II)}$ (24)
60	253 vvw		266 vw	252 w	258	ν (O30–H10) (36), ν (C20–C26) (22), ν (C1–C7) (22)
61		43 vvw			48	ν (O30–H10) (50), ((C20–C26–O30) (13), ((C1–C7–O8) (13)
A_u symmetry						
62	975 sh	975 w	972 vw		972	γ (C3–H12) (38), γ (C22–H28) (34)
63	956 vw	956 w	953 sh		964	γ (C18–H24) (37), γ (C6–H16) (35)
64	934 m		928 m		877	γ (O9–H10) (29), γ (O29–H31) (29), γ (O30–H31) (18) S_{89}, τwis COO (15)
65	839 w	842 m			849	γ (C21–H27) (24), γ (C3–H12) (24)
66	778 sh				813	γ (C19–H25) (30), γ (C6–H16) (29)
67	773 s	774 w			760	γ (C26–O29–O30) (16), γ (C7–O8–O9) (16), $\beta_{R3(I)}$ (16), $\tau_{R1(II)}$ (16)
68	696 m				679	$\beta_{R3(I)}$ (30), $\tau_{R1(II)}$ (30)
69	507 m	503 vvw	503 vw		506	$\tau_{R2(II)}$ (16), $\tau_{R2(I)}$ (16), γ (C17–O23) (16), γ (C4–O13) (16)
70	420 vvw				412	β (C4–O13) (31), γ (C17–O23) (31)
71	357 vvw	355 vvw			353	γ (O23–H32) (48), γ (O13–H14) (46)
72	309 vvw	308 m			292	γ (C7–C1) (17), γ (C26–C20) (17), $\tau_{R2\ (I)}$ (12),$\tau_{R2(II)}$ (12)
73		125 w			114	$\tau_{R2(II)}$ (27), $\tau_{R2(I)}$ (27)
74		85 sh			79	τwis COO(I) (35), τwis COO(II) (18), (18) S_{57}
75		43 vvw			28	τwis COO (49)
76		17 vw			15	γ (O30–H31) (66)
B_g symmetry						
77	975 sh	975 w	972 vw		972	γ (C21–H27) (39), γ (C3–H12) (34)
78	956 vw	956 w	953 sh		963	γ (C6–H16) (38), γ (C19–H25) (36)
79	856 s	855 m	853 s		863	γ (O30–H31) (54), γ (O29–H31) (20), γ (O9–H10) (20)
80	856 s	855 m	853 s		827	ν (C17–O23) (14), ν (C4–C5) (11), ν (C20–C21) (11), ν (C1–C6) (11), ν (C22–C17) (11)
81	832 sh	833 sh		829 w	813	γ (C6–H16) (30), γ (C19–H25) (29)
82	764 sh	765 w			754	γ (C26–O29–O30) (20), γ (C7–O8–O9) (20), ν (C26–O29 (11)
83	696 m				681	$\tau_{R1(II)}$ (31), $\tau_{R1(I)}$ (31)
84	507 m	503 vvw	503 vw		507	$\tau_{R2(I)}$ (16), $\tau_{R2(II)}$ (16), γ (C4–O13) (16), γ (C17–O23) (16)
85	409 vw				411	$\tau_{R3(I)}$ (46), $\tau_{R3(II)}$ (31)
86	357 vvw	355 vvw			353	γ (O13–H14) (48), γ (O23–H32) (46)
87	309 vvw	308 m			297	γ (C7–C1) (17), γ (C26–C20) (17)
88		140 vs			133	$\tau_{R2(I)}$ (24), $\tau_{R2(II)}$ (24), γ (O30–H31) (13)
89		63 vvw			67	τwis COO(I) (44), τwis COO(II) (44)
90		43 vvw			51	γ (O9–H10) (19), γ (O29–H31) (19), γ (O30–H31) (18)

Abbreviations: vs, very strong; s, strong; m, medium; sh, shoulder; w, weak; vvw, very very weak; br, broad. ν, stretching; δ, deformation; ρ or β, rocking or in the plane bending; γ, out-of-plane bending or wagging; τw, twisting. βR, ring deformation; τR, ring torsion. See Fig. 2: Ring (I) and Ring (II).

[a] This work, (sol), solid phase.

[b] Refs. [30,31], (sol), solid phase.

[c] From scaled quantum mechanics force field.

of hydroxybenzoic acid in solid phase the mentioned splittings are also observed. In this case, the bands involved are: 1614/1600, 1453/1446, 1297/1282, 773/764, 643/639, 512/507 and 249/243 cm^{-1}. It is known that even in the 4-hydroxybenzoic acid solid state, exists as H-bonded cyclic dimers [24] and the involving modes of the acid group motions are strongly affected by the double hydrogen bond. The frequencies values in the dimeric species are shifted with respect to the monomers and the splittings of frequencies antisymmetric and symmetric modes are particularly large. The discussion of the

assignment of 4-hydroxybenzoic acid cyclic dimer is performed below.

5.1. Assignments

Region 4000–1900 cm^{-1}. This region is characteristic of the O–H stretching phenolic and acidic groups and C–H stretching of the rings [35,36,38]. The benzoic acid in solid state as dimer exits where the units are bounded by means of hydrogen bonds [40] and gives rise to a very broad band between 3100 and 2500 cm^{-1} [37]. The numerous bands in the IR spectrum of 4-hydroxybenzoic acid also suggest the formation of associates units as dimer [40]. For the hydroxybenzoic acid, Sánchez de La Blanca et al. [30,31] assigned the band at 3385 cm^{-1} to OH stretching phenolic and the band at 3100 cm^{-1} to OH stretching acidic. Our calculations for (II) structure of cyclic dimer using 6-31G* basis set predict the symmetric mode of OH stretching phenolic at practically the same frequency (3746 cm^{-1}) than the antisymmetric mode (3745 cm^{-1}). For this, the ν_1 and ν_{32} modes, respectively are assigned to intense IR band at 3395 cm^{-1} associated to two OH stretching phenolic of the cyclic dimer. The very weak IR band at 3202 cm^{-1} is possibly originated by the coupling of the C=O stretching and OH bending combination bands in agreement with the results obtained for the benzoic acid dimer by Reva and Stepanian [41]. In our case, we assigned that band to the ν_2 and ν_{33} modes, respectively associated to antisymmetric and symmetric C–H stretching in agreement to calculation. The modes from ν_3 to ν_5 and from ν_{34} to ν_{36} associated to the C–H stretching are assigned to the bands in the Raman spectrum at 3160, 3149 and 3087 cm^{-1}, as in Table 8. Some of these modes appear lightly coupled among them as in Table 8. The ν_5 and ν_{36} modes, associated to the symmetric CH stretching, as the theoretical intensity for the symmetric mode predicts are assigned to the medium intensity band in the Raman spectra at 3087 cm^{-1}. Urbanová et al. [38] predict the antisymmetric and symmetric modes corresponding to OH stretching acidic for benzoic acid dimer between 3235 and 3188 cm^{-1} while Stepanian et al. [40] have assigned these modes at 2605 and 2575 cm^{-1}, respectively. Also, in the benzoic acid cyclic dimer [33–38] a strong harmonic coupling between the two OH stretching acidic modes different from 4-hydroxybenzoic acid cyclic dimer was in our case, identified and these modes are strongly shifted by 621 and 520 cm^{-1} (6-31G* basis set) with respect to the monomeric vibration. These shifts are smaller than those found by Antony et al. [33] for the benzoic acid cyclic dimer (836 and 712 cm^{-1}). These authors have demonstrated the importance of anharmonic effects in the OH stretching spectra of carboxylic acid dimers. Here, the antisymmetric and symmetric modes corresponding to OH stretching acidic for (II) structure of cyclic dimer are calculated at 3191 and 3099 cm^{-1}, respectively. The predicted frequencies associated to both OH stretching acidic modes are splited about 92 cm^{-1}, for this, the ν_6 and ν_{37} modes are assigned to the band of medium intensity observed in Raman spectrum at 3054 cm^{-1}. The numerous bands between 2900 and 2400 cm^{-1} in the IR spectrum are characteristic of the hydrogen bonds (Figs. 5 and 6).

Region 1800–1200 cm^{-1}. In this region, the C=C, C–C, C=O, C–O stretchings vibrations are expected, the OH deformation of the phenolic and acidic groups, and also the ring deformations. The PED value (Table 8) clearly shows the strong coupling between these modes in dimer species. In this case, there are two C=O stretching modes, the antisymmetric and symmetric modes. Urbanová et al. [38], Florio et al. [35,36], Antony et al. [33] predict these modes for the benzoic acid dimer between 1786 and 1608 cm^{-1}. Sánchez de La Blanca et al. [30,31] assigned for the 4-hydroxybenzoic acid the shoulder IR at 1685 cm^{-1} and the intense band at 1675 cm^{-1} to antisymmetric C=O stretching of COO group, while the bands in the Raman spectrum (medium) at 1620 cm^{-1} is assigned to symmetric C=O stretching. Our calculations predict the antisymmetric C=O stretching mode at higher frequencies than the symmetric mode (1724 and 1681 cm^{-1}, respectively). For this, the ν_{38} mode is assigned to the very strong band IR at 1678 cm^{-1} related to the antisymmetric C=O stretching mode of the cyclic dimmer, while the ν_7 mode is assigned to intense IR band at 1614 cm^{-1} due to symmetric C=O stretching mode. This last band is also assigned to ν_{39} mode associated to principally C=C stretching. The C=C stretching in the cyclic dimer appears hardly coupled with other modes, such as in the plane C–H deformation modes (βC–H). The ν_8, ν_9 and ν_{40} modes are assigned to intense IR and Raman bands at 1600 cm^{-1} because they are associated to C=C stretching of the cyclic dimer. Urbanová et al. [38] predict the C=C stretching for benzoic acid dimer between 1664 and 1642 cm^{-1} and the βC–H modes between 1545 and 1499 cm^{-1}. Here, the theoretical βC–H modes in the (I) cyclic dimer are predicted at 1567 and 1564 cm^{-1}, while in the (II) structure at 1567 and 1566 cm^{-1}. For this, the ν_{10} and ν_{41} modes are assigned to the weak band in the infrared spectrum at 1511 cm^{-1} due to the in the plane C–H deformation of the cyclic dimer, while the ν_{11} mode, due to the OH symmetric deformation acidic of the cyclic dimer, is assigned to the weak broad band at 1455 cm^{-1}. Sánchez de La Blanca et al. [30,31] have assigned the OH acidic deformation at 1423 cm^{-1}. Thus, the ν_{42} mode is also assigned to the band at 1453 cm^{-1} related to C=C stretching of cyclic dimer. These modes are calculated with the 6-31G* basis set at 1484 and 1482 cm^{-1}. The antisymmetric OH acidic deformation for cyclic dimer is predicted at 1475 cm^{-1}, while in the benzoic acid cyclic dimer it appears in one case at 1474 cm^{-1} [38] and in other case at 1481 cm^{-1} [33]. The ν_{12} and ν_{43} modes are assigned to the IR intense band at 1428 cm^{-1} and are associated to antisymmetric OH deformation acidic and C=C stretching. The ν_{13} and ν_{44} modes related principally to antisymmetric and symmetric OH phenolic deformation could be assigned to the very strong IR band at 1320 cm^{-1} and that appear with medium intensity in the Raman spectrum at 1315 cm^{-1}. Also the ν_{14} and ν_{45} modes, both associated to βC–H modes could be assigned to this last band. In this region, Sánchez de La Blanca et al. [30,31] assigned the shoulder in the IR spectrum at 1315 cm^{-1} to the ring stretching mode. For benzoic acid cyclic dimer, Urbanová et al. [38] and Florio et al. [35,36] have assigned the symmetric and antisymmetric C–O acid stretching between 1359 and 1334 cm^{-1}. In all our theoretical calculations for cyclic dimer, these modes are calculated in cyclic dimer between 1302 and 1319 cm^{-1}. The ν_{15} and ν_{46} modes are assigned to the intense IR band at 1297 cm^{-1} and in the Raman spectrum at 1290 cm^{-1} and both modes associated to C–O stretchings phenolic of the cyclic dimer. The ν_{16} and ν_{47} modes, related to the antisymmetric C–O acidic stretching for cyclic dimer and C=C stretching, respectively are assigned to strong IR band at 1245 cm^{-1}. Sánchez de La Blanca et al. [30,31] assigned to antisymmetric C–O acidic modes at 1291 and 1243 cm^{-1}. The weak IR band observed at 1230 cm^{-1} by Sánchez de La Blanca et al. [30,31] for 4-hydroxybenzoic acid is assigned to ring vibrations. The ν_{17} and ν_{48} modes associated to βC–H modes are assigned to the weak band observed in the Raman spectrum at 1223 cm^{-1}. The OH phenolic deformation mode of phenol in the gas phase spectrum is observed by Michalska et al. [62] at 1343 cm^{-1} and this vibration is strongly coupled with skeletal vibration of the same symmetry gives rise to another band at about 1340 cm^{-1}. Therefore, this band contributes mainly to the fundamental at 1176.5 cm^{-1} and also to the mode at 1343 cm^{-1}. The OH stretching mode in phenol is calculated at 1197 cm^{-1} [61] while Sánchez de La Blanca et al. [30,31] for 4-hydroxybenzoic acid is assigned at higher frequency (1297 cm^{-1}). In our case, the three used theoretical DFT methods perfectly predict both frequencies and forms of these modes, for this, the ν_{18} and ν_{49} modes are easily assigned to the strong bands in the infrared and Raman spectra at 1166 cm^{-1}.

Table 9
Comparison of intermonomers coordinates for 4-hydroxybenzoic acid cyclic dimer with the corresponding of benzoic acid dimer.

Description	Hydroxybenzoic acid[a]							Benzoic acid	
	Mode	6-31G*		D95**		6-311++G**		6-31G** [b,c]	D95** [d]
		I	II	I	II	I	II		
νs (O–H···O)	ν30	49	49	51	51	48	48	120	121
νa (O–H···O)	ν61	111	111	113	113	106	106	107	107
δ(OH···O)	ν31	97	97	97	97	96	95	65	65
γs (OH···O)	ν76	55	55	56	56	53	52	61	61
Twisting	ν75	33	33	36	36	34	32	35	32
γa (OH···O)	ν90	17	17	19	19	18	15	18	19

[a] This work.
[b] Ref. [35].
[c] Ref. [36].
[d] Ref. [33].

Region 1200–1000 cm^{-1}. In this region the modes expected such as C–C stretching, C–H in the plane deformation, C–H out-of-plane deformation, ring deformations, ring torsion appear strongly coupled. For cyclic dimmer, the two C–O stretching modes are predicted at 1162 and 1158 cm^{-1}. Again, there is a slightly shifting of these modes between approximately 49 and 40 cm^{-1} with respect to the monomeric vibration. The two modes associated to C–O stretching acidic (ν_{19} and ν_{50} modes) are assigned to the weak IR band at 1133 cm^{-1} and of medium intensity at 1132 cm^{-1}. The ν_{20} and ν_{51} modes related to βC–H modes are assigned to the medium intensity band in the infrared spectrum at 1107 cm^{-1} and observed as very weak in the Raman spectrum. The ν_{21} and ν_{52} modes associated to the ring deformation cyclic dimer (βR_1) are calculated at 1031 cm^{-1} and for this reason; those modes are assigned to the weak IR bands at 1020 cm^{-1}. These assignments are in agreement with Sánchez de La Blanca et al. [30,31].

Region 1000–10 cm^{-1}. In this region, the C–H wagging modes with A_u symmetry are expected and they are easily characterized by B3LYP/6-31G* calculation. For this, the ν_{62}, ν_{63}, ν_{65} and ν_{66} modes are assigned to the bands at 975, 956, 839 and 778 cm^{-1}. These assignments are in accordance with those previously reported by Sánchez de La Blanca et al. [30,31]. The only mode predicted with B_u symmetry (ν_{53}) is assigned to strong IR band at 856 cm^{-1}. The most important observation in this region is the strong shift predicted for the COH out-of-plane bending acidic (γOH vibration) for cyclic dimer from 599 cm^{-1} in the monomers to 961 and 911 cm^{-1} in the dimer, as shown in Tables S4 and S5. Such observation is essentially caused by an effective stiffening of the bending motion due to hydrogen bond. The γOH mode of the monomer exhibits an extreme shift upon dimerization (ν_{64} and ν_{79}). These results are similar to those obtained for benzoic acid cyclic dimer [33–41]. Antony et al. [33] could not satisfactorily explain this behavior by their nonperturbative results. They have anticipated that at least four-dimensional calculations are required to finally clarify the question of the anharmonic effect on γOH mode of the benzoic acid dimer. However, either of these approaches is currently beyond the available computational means. For hydroxybenzoic acid Sánchez de La Blanca et al. [30,31] have assigned the γOH modes at 928 cm^{-1}. In our case, the higher PED values perfectly predict the two modes and for this, the ν_{64} and ν_{79} modes associated to the γOH modes for the cyclic dimer are assigned to the mediun intensity IR band at 934 cm^{-1} and the strong band at 856 cm^{-1}, respectively. For hydroxybenzoic acid, in the region 792–647 cm^{-1} Sánchez de La Blanca et al. [30,31] did not observed any band. In this case, the theoretical calculations for hydroxybenzoic acid cyclic dimer predicts the two γ(COO) modes at 772 cm^{-1}, whereas only one δ(COO) mode at 771 cm^{-1}. The other δ(COO) mode appears coupled with other modes at 624 cm^{-1}. For this, the ν_{67} and ν_{54} modes associated to γ(COO) modes of cyclic dimer are assigned to the intense IR band at 773 cm^{-1} and at 774 cm^{-1} in the Raman spectrum and the shoulder at 764 cm^{-1}. The C–C stretching mode related to the ν_{23} mode and the ν_{82} mode associated to δ(COO) mode for cyclic dimer could be assigned to the band at 764 cm^{-1}. The ν_{25} mode associated to the remaining δ(COO) mode of A_g symmetry is assigned to the strong band localized at 620 cm^{-1} in the IR spectrum, as the PED value predicts. For cyclic dimer, the calculation results predict in this region some torsion (τR) and ring deformations (βR) modes. Sánchez de La Blanca et al. [30,31] assigned the very weak IR bands at 691 and 640 cm^{-1} to ring modes. Because of that, the ν_{68} and ν_{83} modes associated to τR_1, ν_{55} mode (βR_3) and ν_{56} mode (βR_2) are assigned to set of IR bands at 696, 644 and 596 cm^{-1}, respectively. For hydroxybenzoic acid, Sánchez de La Blanca et al. [30,31] assigned the medium intensity IR bands at 617 and 546 cm^{-1} to symmetric and antisymmetric δ(COO) modes. In our case, the rocking modes of COOH groups for cyclic dimer are predicted at 557 and 524 cm^{-1}. For this, the medium intensity IR band at 550 cm^{-1} and the Raman band at 521 cm^{-1} are assigned to these modes for cyclic dimer (ν_{26} and ν_{57}). In phenol, the in plane C–O deformation mode (βC–O) is calculated at 410 cm^{-1}, whereas Sánchez de La Blanca et al. [30,31] do not consider this mode in their assignation. Our calculations predict that mode for cyclic dimer at 417 and 408 cm^{-1}. Because of that the IR bands at 420 and 401 cm^{-1} are assigned to those modes (ν_{27} and ν_{70}). Moreover, the out-of-plane COH bendings phenolic (γOH vibration) are predicted with A_u and B_g symmetries. For this reason, the two modes (ν_{71} and ν_{86}) are assigned to a very weak band at 357 cm^{-1}. Here again, we can see as the band related to OH phenolic group does not change respect to monomers because these OH groups are not involved in the formation of cyclic dimer.

In this low region, in the Raman spectrum of hydroxybenzoic acid many bands are observed with higher intensity, this fact probably is due to additional resonance interactions. In the benzoic acid studied by Florio et al. [36] they have observed as a consequence of the fact that normal mode OH bend vibrations of cyclic dimer have contributions from both the OH and CH bends. This leads to a sharing of intensities over many states, which fills in the lower frequency region of the spectrum for benzoic acid dimer. Other cause would be the observed by Reva and Stepanian [41] in the same cyclic dimer, the other more strongly H-bonded dimer may have more substantial contributions from the coupling of the OH stretch with the intermolecular stretch. The calculations predicted the intermonomers modes for cyclic dimmer in the lower region of the spectrum. These modes were not characterized by Sánchez de La Blanca et al. [30,31] for hydroxybenzoic acid.

5.2. Intermonomer modes

In the 270–10 cm^{-1} region the intermonomer vibrational modes of the dimer [32–40] appear related to restricted translations or

rotations of one molecule against the other (see Table 2). Table 9 shows the theoretical frequencies and assignments of the intermonomer vibrational modes for cyclic dimer compared with the calculated ones for the benzoic acid cyclic dimer. Florio et al. [35,36] and Alcolea Palafox et al. [37] have obtained for all intermonomer vibrational modes of benzoic acid cyclic dimer the same frequencies using B3LYP/6-31G** method, while Antony et al. [33] have obtained little difference in many modes using B3LYP/D95** method. In our case, the six intermonomer modes appear strongly coupled with other modes, as shown in Table 8 and all modes are only observed in the Raman spectrum. The PED value shown of symmetric OH–O stretching mode (ν_{30}) shows a slightly coupling with the OH–O deformation mode (ν_{31}), while the antisymmetric OH–O stretching mode appears strongly coupled with other modes. The calculated spectrum predicts the two OH–O stretching modes at 111 and 49 cm^{-1} respectively, but with greater intensity for the symmetrical mode. For this reason, the ν_{30} mode, associated to symmetrical mode is assigned to the very strong Raman band at 111 cm^{-1}, while the ν_{61} mode is assigned to the strong band in the same spectrum and it is related to the antisymmetric mode. For benzoic acid cyclic dimer, the two symmetrical and antisymmetric γ(O–H–O) modes are calculated at 61 and 18 cm^{-1}, while in our calculations using the same method, they are calculated at 55 and 17 cm^{-1}, respectively (ν_{76} and ν_{90}). Other similar variation between both cyclic dimers is found for the calculated δ(O–H–O) mode (ν_{31}) by us, using all basis sets at 97 cm^{-1}, while in the cyclic dimer of benzoic acid it is calculated with other basis sets at 65 cm^{-1}. Finally, the calculated frequencies for the twisting mode (ν_{75}) with the three basis sets is 33 cm^{-1}, while for cyclic dimer of benzoic acid it is calculated at 35 cm^{-1}.

6. Conclusions

- The present study shows that considering four structures for the monomers and two structures for the 4-hydroxybenzoic acid cyclic dimer, the II structure is more stable in two cases.
- Our vibrational analysis of 4-hydroxybenzoic acid is based on DFT/B3LYP calculations using 6-31G* basis set and the analysis of the IR and Raman spectra were realized considering the most stable II structure for the cyclic dimer.
- The present study confirms the assignments previously made [30,31] with some modifications indicated by the most accurate force field developed in the present work. Also, the assignment of the intermonomer vibrational modes for most stable cyclic dimer is carried out and the assignments of the 90 normal modes of vibration corresponding to 4-hydroxybenzoic acid cyclic dimer are reported.
- The complete force field for cyclic dimer has been determined, as well as the principal force constants for stretching and deformation modes.
- The present work reveals the existence of intermolecular contacts between adjacent molecules in the crystal, as was observed in solid phase. Those intermolecular contacts have been interpreted by NBO and topological analysis calculations.

Acknowledgments

We acknowledge research grants from CIUNT (Consejo de Investigaciones de la Universidad Nacional de Tucumán) and CONICET (Consejo Nacional de Investigaciones Científicas y Técnicas, PIP 0629). S. A. Brandán thanks the Beca Banco Rio for a grant supporting this work. The autors thank Prof. Tom Sundius his permission for using MOLVIB.

Appendix A. Supplementary data

Supplementary data associated with this article can be found, in the online version, at doi:10.1016/j.saa.2010.01.012.

References

[1] D. Boskou, Olive Oil, Chemistry and Technology, ADSL Press, Champagn, IL, USA, 1996.
[2] A. Serrano, C. Palacios, G. Roy, C. Cespón, M.L. Villar, M. Nocito, P. González-Porqué, Arch. Biochem. Biophys. 350 (1998) 49.
[3] F.A.M. Silva, F. Borges, M.A. Ferreira, J. Agric. Food Chem. 49 (2001) 3936.
[4] A.P. Vafiadis, E.G. Bakalbassis, Chem. Phys. 195 (2005) 204.
[5] O.I. Aruoma, A. Murcia, J. Butler, B. Halliwell, J. Agric. Food Chem. 41 (1993) 1880.
[6] C.A. Rice-Evans, N.J. Miller, G. Paganga, Free Radic. Biol. Med. 20 (1996) 933.
[7] G. Cao, E. Sofic, R.L. Prior, Free Radic. Biol. Med. 22 (1997) 749.
[8] H. Esterbauer, J. Gebicki, H. Puhl, G. Jurgens, Free Radic. Biol. Med. 13 (1992) 341.
[9] B. Halliwell, J.C. Gutteridge, Free Radicals in Biology and Medicine, Oxford Science Publications, 1999.
[10] S. Passi, M. Picardo, M. Nazzaro-Porro, Biochem. J. 245 (1987) 537.
[11] T. Nakayama, Cancer Res. 54 (1994) 1991.
[12] E. Sergediene, K. Jonsson, H. Szymusiak, B. Tyrakowska, I.M. Rietjens, N. Cenas, FEBS Lett. 462 (1999) 392.
[13] M. Inoue, N. Sakaguchi, K. Isuzugawa, H. Tani, Y. Ogihara, Biol. Pharm. Bull. 23 (2000) 1153.
[14] G. Roy, M. Lombardia, C. Palacios, A. Serrano, C. Cespón, E. Ortega, P. Eiras, S. Lujan, Y. Revilla, P. González-Porqueĭ, Arch. Biochem. Biophys. 383 (2000) 206.
[15] T. Gao, Y. Ci, H. Jian, C. An, Vib. Spectrosc. 24 (2000) 225.
[16] C.A. Gomes, T. Giraöda Cruz, J.L. Andrade, N. Milhazes, F. Borges, M.P.M. Marques, J. Med. Chem. 46 (2003) 5395.
[17] R. Ikeda, J. Sugihara, H. Uyama, S. Kobayashi, Polym. Int. 47 (1998) 295.
[18] J. Huth, T. Mosell, K. Nicklas, A. Sariban, J. Brickmann, J. Phys. Chem. 98 (1994) 7685.
[19] B.M. Kariuki, C.L. Bauer, K.D.M. Harris, S.J. Teat, Angew. Chem. 39 (24) (2000) 4486.
[20] T. Imase, S. Kawauchi, J. Watanabe, Macromol. Theory Simul. 10 (5) (2001) 434.
[21] M. Nolan, J.C. Greer, J. Phys. Chem. B 103 (34) (1999) 7111.
[22] P.I. Nagy, W.J. Dunn, G. Alagona, C. Ghio, J. Phys. Chem. 97 (1993) 4628.
[23] E.A. Heath, P. Singh, Y. Ebisuzaki, Acta Crystallogr. C 48 (1992) 1960.
[24] M. Colapietro, A. Domenicano, C. Marciante, Acta Crystallogr. B 35 (1979) 2177.
[25] T.J. Hsieh, C.C. Su, C.Y. Chen, C.H. Liou, L.H. Lu, J. Mol. Struct. 741 (2005) 193.
[26] J. Fang-Fang, Z. Pu-Su, W. Qing-Xiang, Phys. Org. Chem. 24 (2) (2005) 184.
[27] W. Liyuan, Y. Shangxian, J. Photop, Sci. Technol. 12 (2) (1999) 331.
[28] R. Sabbah, M. Gouali, Thermochim. Acta (1997) 107.
[29] L. Ran Wang, Y. Fang, Spectrochim. Acta Part A 62 (2005) 958.
[30] E. Sánchez De La Blanca, J.L. Nuñez, P. Martínez, Anales de Química 82 (1986) 480.
[31] E. Sánchez De La Blanca, J.L. Nuñez, P. Martínez, An. Quím. 82 (1986) 490.
[32] S.F. Boys, F. Bernardi, Mol. Phys. 19 (1973) 553.
[33] J. Antony, G. Von Helden, G. Meijer, B. Schmidt, J. Chem. Phys. 123 (2005) 14305.
[34] M.R. Johnson, H.P. Trommsdor, Chem. Phys. Lett. 364 (2002) 34.
[35] G.M. Florio, E.L. Sibert, T.S. Zwier, Faraday Discuss. 118 (2001) 315.
[36] G.M. Florio, T.S. Zwier, E.M. Myshakin, K.D. Jordan, E.L. Sibert, J. Chem. Phys. 118 (4) (2003) 1735.
[37] M. Alcolea Palafox, J.L. Nuñez, M. Gil, Int. J. Quant. Chem. 89 (2002) 1.
[38] M. Urbanová, V. Setnic¡ka, F.J. Devlin, P.J. Stephens, J. Am. Chem. Soc. 127 (2005) 6700.
[39] M. Plazanet, N. Fukushima, M.R. Johnson, A.J. Horsewill, H.P.J. Trommsdorff, Chem. Phys. 115 (7) (2001) 3241.
[40] S.G. Stepanian, I.D. Reva, E.D. Radchenko, G.G. Sheina, Vib. Spectrosc. 11 (1996) 123.
[41] I.D. Reva, S.G. Stepanian, J. Mol. Struct. 349 (1995) 337.
[42] J. Fang-Fang, Z. Pu-Su, W. Qing-Xiang, Chin. J. Struct. Chem. 24 (2) (2005) 184.
[43] R.F.W. Bader, Atoms in Molecules—A Quantum Theory, Oxford University Press, Oxford, 1990, ISBN: 0198558651 (Available on-line from amazon.com).
[44] F. Biegler-König, J. Schönbohm, D. Bayles, AIM2000: a program to analyze and visualize atoms in molecules, J. Comput. Chem. 22 (2001) 545.
[45] U. Koch, P.L.A. Popelier, J. Phys. Chem. 99 (1995) 9747.
[46] A.E. Reed, L.A. Curtiss, F. Weinhold, Chem. Rev. 88 (1988) 899.
[47] J.P. Foster, F. Weinhold, J. Am. Chem. Soc. 102 (1980) 7211.
[48] A.E. Reed, F. Weinhold, J. Chem. Phys. 83 (1985) 1736.
[49] E.D. Glendening, A.E. Reed, J.E. Carpenter, F. Weinhold, NBO Version 3.1.
[50] R. Dennington II, Todd Keith, J. Millam, K. Eppinnett, W. Lee Hovell, R. Gilliland, GaussView, Version 3.0, Semichem, Inc., Shawnee Mission, KS, 2003.
[51] M.J. Frisch, G.W. Trucks, H.B. Schlegel, G.E. Scuseria, M.A. Robb, J.R. Cheeseman, J.A. Montgomery Jr., T. Vreven, K.N. Kudin, J.C. Burant, J.M. Millam, S.S. Iyengar, J. Tomasi, V. Barone, B. Mennucci, M. Cossi, G. Scalmani, N. Rega, G.A. Petersson, H. Nakatsuji, M. Hada, M. Ehara, K. Toyota, R. Fukuda, J. Hasegawa, M. Ishida, T. Nakajima, Y. Honda, O. Kitao, H. Nakai, M. Klene, X. Li, J.E. Knox, H.P. Hratchian, J.B. Cross, V. Bakken, C. Adamo, J. Jaramillo, R. Gomperts, R.E. Stratmann, O. Yazyev, A.J. Austin, R. Cammi, C. Pomelli, J.W. Ochterski, P.Y. Ayala, K. Morokuma, G.A. Voth, P. Salvador, J.J. Dannenberg, V.G. Zakrzewski, S. Dapprich,

A.D. Daniels, M.C. Strain, O. Farkas, D.K. Malick, A.D. Rabuck, K. Raghavachari, J.B. Foresman, J.V. Ortiz, Q. Cui, A.G. Baboul, S. Clifford, J. Cioslowski, B.B. Stefanov, G. Liu, A. Liashenko, P. Piskorz, I. Komaromi, R.L. Martin, D.J. Fox, T. Keith, M.A. Al-Laham, C.Y. Peng, A. Nanayakkara, M. Challacombe, P.M.W. Gill, B. Johnson, W. Chen, M.W. Wong, C. Gonzalez, J.A. Pople, Gaussian 03, Revision C. 02, Gaussian, Inc., Wallingford, CT, 2004.
[52] T.H. Dunning Jr., J. Chem. Phys. 53 (1970) 2823.
[53] T.H. Dunning Jr., J. Chem. Phys. 90 (1989) 1007.
[54] T. Sundius, J. Mol. Struct. 218 (1990) 321.
[55] T. Sundius, MOLVIB: A Program for Harmonic Force Field Calculation, QCPE Program No. 604, 1991.
[56] G. Fogarasi, P. Pulay, in: J.E. Durig (Ed.), Vibrational Spectra and Structure, vol. 14, Elsevier, Amsterdam, 1985, p. 125.
[57] G. Rauhut, P. Pulay, J. Phys. Chem. 99 (1995) 3093.
[58] G. Rauhut, P. Pulay, J. Phys. Chem. 99 (1995) 14572.
[59] F. Kalincsák, G. Pongor, Spectrochim. Acta A 58 (2002) 999.
[60] P.L.A. Popelier, J. Phys. Chem. A 102 (1998) 1873.
[61] G. Keresztury, F. Billes, M. Kubinyi, T. Sundius, J. Phys. Chem. A 102 (1998) 1371.
[62] D. Michalska, D.C. Bienko, A.J. Abkowicz-Bienko, Z. Latajka, J. Phys. Chem. 100 (1996) 17786.